Research article JHEP|Reports

An immunoassay system to investigate epidemiology of *Rocahepevirus ratti* (rat hepatitis E virus) infection in humans

Authors

Jianwen Situ, **Kelvin Hon-Yin Lo**, **Jian-Piao Cai**, Zhiyu Li, Shusheng Wu, Estie Hon-Kiu Shun, Nicholas Foo-Siong Chew, James Yiu-Hung Tsoi, Gabriel Sze-Man Chan, Winson Hei-Man Chan, Cyril Chik-Yan Yip, Kong Hung Sze, Vincent Chi-Chung Cheng, Kwok-Yung Yuen, Siddharth Sridhar

Correspondence

sid8998@hku.hk (S. Sridhar).

Graphical abstract

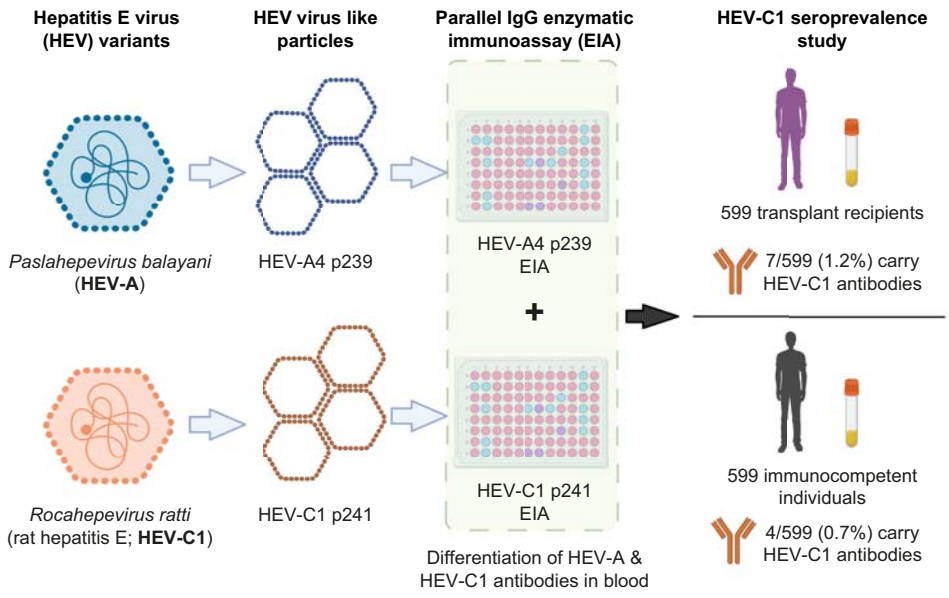

Highlights

- Rat hepatitis E virus (HEV-C1) is an emerging divergent cause of human hepatitis E.
- HEV-A4 p239 and HEV-C1 p241 ORF2 truncated peptides form virus-like particles (VLPs).
- An enzymatic immunoassay (EIA) for HEV-C1 was designed with these VLPs.
- The EIA differentiates HEV-C1 and other hepatitis E variant serum antibody profiles.
- The validated EIA was used for the first HEV-C1 seroprevalence estimate in humans.

https://doi.org/10.1016/j.jhepr.2023.100793

Impact and Implications

Rat hepatitis E virus has recently been discovered to infect humans, but antibody tests for this infection are lacking, making it difficult to gauge how common this infection is. We developed an antibody test algorithm that can identify individuals with past rat hepatitis E virus exposure. We used this algorithm to estimate rat hepatitis E exposure rates in humans in Hong Kong and found that approximately 1% of all tested people had been exposed to this virus previously.

Research article

JHEP|Reports

An immunoassay system to investigate epidemiology of *Rocahepevirus ratti* (rat hepatitis E virus) infection in humans

Jianwen Situ,[1,†] **Kelvin Hon-Yin Lo**,[1,†] **Jian-Piao Cai**,[1,†] Zhiyu Li,[1] Shusheng Wu,[1] Estie Hon-Kiu Shun,[1] Nicholas Foo-Siong Chew,[1] James Yiu-Hung Tsoi,[1] Gabriel Sze-Man Chan,[1] Winson Hei-Man Chan,[1] Cyril Chik-Yan Yip,[1] Kong Hung Sze,[1] Vincent Chi-Chung Cheng,[1] Kwok-Yung Yuen,[1,2,3,4,5] Siddharth Sridhar[1,2,3,*]

[1]*Department of Microbiology, School of Clinical Medicine, Li Ka Shing Faculty of Medicine, The University of Hong Kong, Pokfulam, Hong Kong, China;* [2]*State Key Laboratory of Emerging Infectious Diseases, The University of Hong Kong, Hong Kong, China;* [3]*Carol Yu Centre for Infection, The University of Hong Kong, Hong Kong, China;* [4]*The Collaborative Innovation Center for Diagnosis and Treatment of Infectious Diseases, The University of Hong Kong, Hong Kong, China;* [5]*Centre for Virology, Vaccinology and Therapeutics, Hong Kong Science and Technology Park, Hong Kong Special Administrative Region, Hong Kong, China*

JHEP Reports **2023.** https://doi.org/10.1016/j.jhepr.2023.100793

Background & Aims: Rat hepatitis E virus (*Rocahepevirus ratti*; HEV-C1) is an emerging cause of hepatitis E that is divergent from conventional human-infecting HEV variants (*Paslahepevirus balayani*; HEV-A). Validated serological assays for HEV-C1 are lacking. We aimed to develop a parallel enzymatic immunoassay (EIA) system that identifies individuals with HEV-C1 exposure. We also aimed to conduct the first HEV-C1 seroprevalence study in humans using this validated EIA system.
Methods: Expressed HEV-A (HEV-A4 p239) and HEV-C1 (HEV-C1 p241) peptides were characterised. Blood samples were simultaneously tested in HEV-A4 p239 and HEV-C1 p241 IgG EIAs. An optical density (OD) cut-off-based interpretation algorithm for identifying samples seropositive for HEV-A or HEV-C1 was validated using RT-PCR-positive infection sera. This algorithm was used to measure HEV-C1 seroprevalence in 599 solid organ transplant recipients and 599 age-matched immunocompetent individuals.
Results: Both peptides formed virus-like particles. When run in HEV-A4 p239 and HEV-C1 p241 EIAs, HEV-A and HEV-C1 RT-PCR-positive samples formed distinct clusters with minimal overlap in a two-dimensional plot of optical density values. The final EIA interpretation algorithm showed high agreement with RT-PCR results (Cohen's $\kappa = 0.959$) and was able to differentiate HEV-A and HEV-C1 infection sera with an accuracy of 94.2% (95% CI: 85.8–98.4%). HEV-C1 IgG seroprevalence was 7/599 (1.2%) among solid organ transplant recipients and 4/599 (0.7%) among immunocompetent individuals. Five of 11 (45.5%) of these patients had history of transient hepatitis of unknown cause.
Conclusions: HEV-C1 exposure was identified in 11/1198 (0.92%) individuals in Hong Kong indicating endemic exposure. This is the first estimate of HEV-C1 seroprevalence in humans. The parallel IgG EIA algorithm is a valuable tool for investigating epidemiology and risk factors for HEV-C1 infection.
Impact and Implications: Rat hepatitis E virus has recently been discovered to infect humans, but antibody tests for this infection are lacking, making it difficult to gauge how common this infection is. We developed an antibody test algorithm that can identify individuals with past rat hepatitis E virus exposure. We used this algorithm to estimate rat hepatitis E exposure rates in humans in Hong Kong and found that approximately 1% of all tested people had been exposed to this virus previously.

Introduction

Hepatitis E virus (HEV) is an important cause of viral hepatitis. 'HEV' is an umbrella term for a large group of RNA viruses in the family *Hepeviridae*. Most members of this family belong to the subfamily *Orthohepevirinae* and circulate in terrestrial animals. *Orthohepevirinae* comprises four genera of which *Paslahepvirus* (species *balayani*; HEV-A) is the most relevant to human health.[1] Of the eight genotypes currently recognised within HEV-A, three cause the bulk of human hepatitis E.[2] HEV-A genotype 1 circulates in humans and spreads by faeco-oral transmission whereas HEV-A genotypes 3 and 4 circulate in swine and infect humans consuming undercooked pork.[3]

The other genera within *Orthohepevirinae* (*Avihepevirus, Rocahepevirus,* and *Chirohepevirus*) were previously considered to have limited zoonotic potential. However, we discovered that *Rocahepevirus* species *ratti* genotype 1 (HEV-C1, known as rat hepatitis E virus) can infect humans.[4] HEV-C1 is an ubiquitous pathogen of street rats

Keywords: HEV-C1; *Orthohepevirus* species C; *Rocahepevirus ratti*; Seroepidemiology; Antibody assay; VLP.
Received 25 August 2022; received in revised form 23 March 2023; accepted 14 April 2023; available online 15 May 2023
† These authors contributed equally.
* Corresponding author. Address: Department of Microbiology, School of Clinical Medicine, Li Ka Shing Faculty of Medicine, The University of Hong Kong, Queen Mary Hospital, 102 Pokfulam Road, Hong Kong, China. Tel.: +00-852-22552408; fax: +00-852-28551241
E-mail address: sid8998@hku.hk (S. Sridhar).

that is highly divergent to HEV-A.[5] Through population-wide surveillance of patients with hepatitis using reverse-transcription PCR (RT-PCR), we have identified 16 HEV-C1-infected persons in Hong Kong, accounting for 8–15% of virologically confirmed hepatitis E cases in the city from 2017 to 2020.[6,7] HEV-C1 infection cases have also been documented in Spain (autochthonous infections) and Canada (in a returning traveller from central Africa), suggesting a global presence of this zoonosis.[8,9] However, other studies in Europe could not identify any HEV-C1 RT-PCR-positive patients in small patient cohorts.[10–12] The true global prevalence of human HEV-C1 infection is uncertain.

RT-PCR is inefficient for studying HEV-C1 prevalence because it requires participants to be actively infected at the time of testing. Assessing community burden of HEV-C1 requires serological tests. Such tests would enable population-wide HEV-C1 seroprevalence studies and identification of risk factors for the infection. However, no commercially available tests are currently available for this purpose. Indeed, we have found that HEV-A based enzymatic immunoassays (EIAs) are often insensitive for HEV-C1 infection.[13]

To address this gap, we developed two peptides: HEV-A4 p239 and HEV-C1 p241 (based on HEV-A genotype 4 and HEV-C1, respectively) and previously provided proof-of-concept that an immunoblot system based on these peptides was capable of detecting HEV-C1 antibodies in human sera.[13] However, immunoblots are cumbersome, difficult to interpret and poorly suited for large-scale high-throughput screening. In this study, we describe a parallel immunoglobulin G (IgG) EIA system that can simultaneously detect HEV antibodies and differentiate between individuals with HEV-A exposure and HEV-C1 exposure. We applied this system to solid organ transplant (SOT) recipients and immunocompetent patient cohorts to measure HEV-C1 IgG seroprevalence in these groups. SOT recipients were specifically chosen for evaluation given relatively high frequency of HEV-C1 infection in this group in Hong Kong.[7]

Patients and methods

Study setting and patient samples

The study was conducted at the Department of Microbiology of Queen Mary Hospital (QMH) in collaboration with Public Health Laboratory Services Branch (PHLSB), the hepatitis reference laboratory for Hong Kong. We used patient serum or plasma samples archived at these two centres between January 1, 2017 and December 31, 2021. Serum or plasma samples testing positive for HEV-A (n = 59) or HEV-C1 (n = 16) by genus-specific RT-PCR assays were retrieved for evaluation of the parallel IgG EIA system. This archive of 16 HEV-C1 patient sera comprises samples from 80% of all patients with HEV-C1 reported globally to date. Potential organ donor sera (n = 290) with undetectable HEV-A/HEV-C1 RNA by RT-PCR and also testing negative for HEV IgG by a commercial antibody assay (Wantai, Beijing, China) were used as negative controls.[13] Once the interpretation algorithm was fully validated, the parallel IgG EIA system was used to measure and compare HEV-C1 seroprevalence in age-matched immunocompromised and immunocompetent adults. The immunocompromised cohort comprised SOT recipients sending blood to QMH for cytomegalovirus monitoring whereas the immunocompetent group comprised outpatients sending blood to QMH for miscellaneous serological tests. Inclusion/exclusion criteria for these two cohorts and matching process are described in the supplementary methods. Sample collection for HEV RT-PCR and serological tests was approved by the Institutional Review Board of the University of Hong Kong/Hospital Authority Hong Kong West Cluster (UW 18-074).

HEV-A4 p239 and HEV-C1 p241 peptide expression and characterisation

Cloning and expression of truncated HEV-A genotype 4 and HEV-C1 open reading frame 2 (ORF2) peptides (termed HEV-A4 p239 and HEV-C1 p241, respectively) was performed as described previously.[13] Genotype 4 is the prevalent HEV genotype in China and belongs to the same serotype as other HEV-A genotypes.[14] HEV-A4 p239 and HEV-C1 p241 encompass major neutralising epitopes of HEV-A and HEV-C1 ORF2, respectively, in the protruding 'P' domain (Fig. 1A). Amino acid sequence alignments of both peptides are presented in Fig. S1A. Peptides were characterised using SDS-PAGE, transmission electron microscopy, and liquid chromatography with tandem mass spectrometry (LC MS-MS). Detailed protocols for peptide expression and characterisation procedures are described in the supplementary material.

HEV-A4 p239 and HEV-C1 p241 parallel IgG immunoblots and EIAs

Control material for initial checkerboard assays for optimising the EIAs were chosen based on HEV-A4 p239 and HEV-C1 p241 immunoblot assays.[13] A brief protocol for the immunoblot assays is included in the supplementary material. These samples were deployed in checkerboard assays to evaluate the optimal antigen coating concentrations and sample dilutions for the HEV-A4 p239 and HEV-C1 p241 EIAs. Optimised HEV-A4 p239 and HEV-C1 p241 EIAs were then evaluated with the panel of HEV-A or HEV-C1 RT-PCR-positive patient blood samples. Samples were run in parallel in both EIAs and optical density (OD) values were measured at 450 nm and 620 nm. OD cut-offs were established for both EIAs individually. An interpretation algorithm for assessing both EIA results in parallel for any given sample was evaluated for its ability to differentiate between HEV-A and HEV-C1 RT-PCR positive sera/plasma. EIA protocols, statistical methods to establish cut-offs, and quality control mechanisms are described in the supplementary methods.

Commercial EIAs and reference sera

The Wantai HEV IgG assay was used because we have previously shown that it has good sensitivity for both HEV-A and HEV-C1 infections although it is unable to differentiate between HEV-A or HEV-C1 patient sera.[13] WHO reference HEV antiserum was procured from NIBSC (code 95/584, Potters Bar, UK). This reference serum was used to assess linearity of IgG EIA assays as previously described.[15]

HEV RT-PCR assays

HEV-A and HEV-C1 real-time RT-PCR assays were performed as described previously.[4] A nested real-time HEV-C1 RT-PCR assay with higher analytical sensitivity was performed on samples testing positive for HEV-C1 antibodies in the seroprevalence study.[13] Primers, targets, and performance characteristics of RT-PCR assays are described in Table S1.

Statistical analysis

The Wilcoxon matched-pairs signed rank test and Mann–Whitney *U* test were used for inter-group comparisons as appropriate. McNemar's test was used to compare sensitivities of the parallel IgG EIA system and Wantai IgG. Proportions were compared with the X^2 test or Fisher's exact test as appropriate.

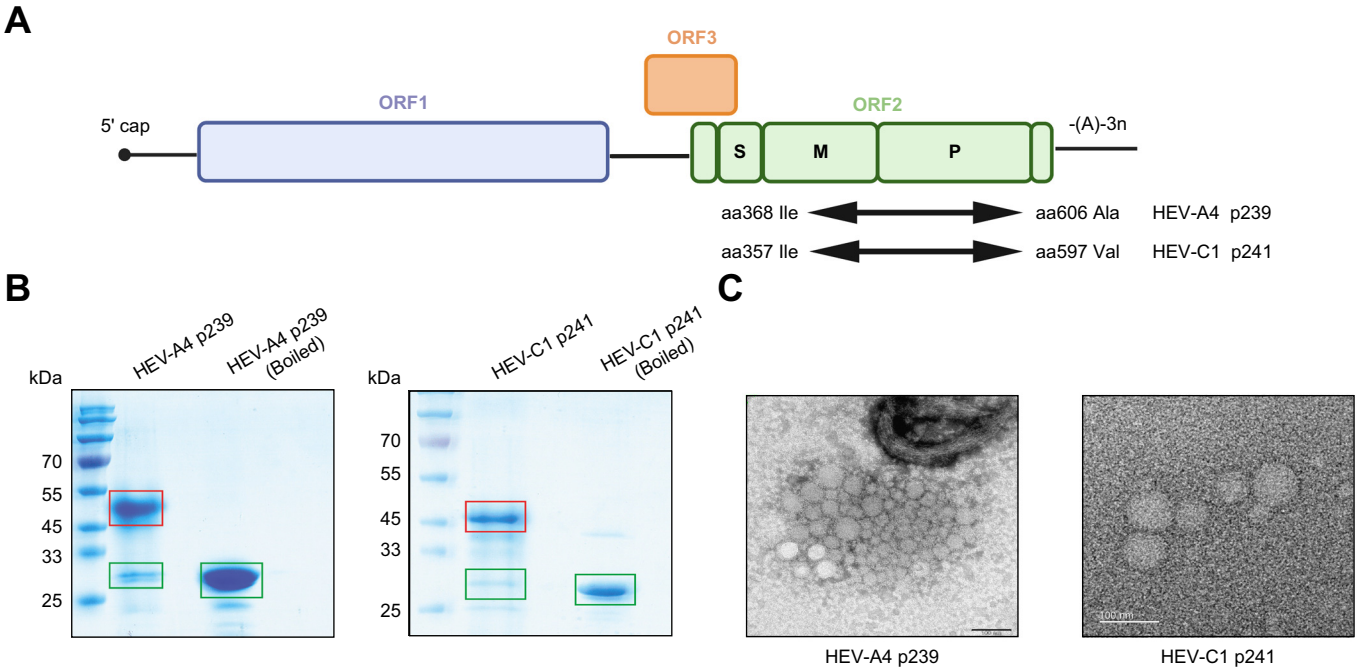

Fig. 1. Characterisation of HEV-A4 p239 and HEV-C1 p241 peptides. (A) Schematic of hepatitis E virus (HEV) genome showing segment encoding HEV-A4 p239 and HEV-C1 p241 peptides. S, M, and P represent regions encoding shell, middle, and protruding domains of ORF2 respectively. (B) SDS-PAGE of HEV-A4 p239 and HEV-C1 p241 peptide dimers (red boxes) showing complete resolution to monomers (green boxes) upon boiling. (C) Electron micrographs of HEV-A4 p239 and HEV-C1 p241 showing virus-like particles. HEV-A, *Paslahepevirus balayani*; HEV-C1, *Rocahepevirus ratti*; ORF2, open reading frame 2.

Figures were generated using Prism (GraphPad, La Jolla, USA) and RStudio (version 1.2.5033, RStudio Inc., Boston, MA, USA). For the seroprevalence study sample size calculation, we estimated general population HEV-C1 IgG seroprevalence at 1.5% assuming that it is one-tenth of the known overall HEV IgG seroprevalence of 15.5% (based on the relative proportion of HEV-C1 and HEV-A RT-PCR confirmed cases in Hong Kong from 2017 to 2020).[6,7,16]

Our hypothesis was that HEV-C1 IgG seroprevalence among SOT recipients is higher at 4.5% (because of a high proportion of SOT recipients among HEV-C1 infection cases in Hong Kong). Based on these parameters, a sample size of 1,016 (508 in SOT group and 508 in immunocompetent group) could identify a 3% difference in HEV-C1 seroprevalence between groups with α = 0.05 and power = 80%.

Results

Characterisation of HEV-A4 p239 and HEV-C1 p241 peptides

The ORF2 protein constitutes the outer capsid of HEV. HEV-A4 p239 and HEV-C1 p241 are N-terminal truncated peptide fragments that incorporate P domains of HEV-A genotype 4 and HEV-C1 ORF2, respectively (Fig. 1A). Despite being derived from homologous regions, these two peptides only share 54.8% identity and are phylogenetically distinct reflecting the considerable antigenic divergence of HEV-A and HEV-C1 (Fig. S1). On SDS-PAGE, both peptides formed prominent bands at 45–50 kDa that resolved into 28 kDa monomers upon boiling (Fig. 1B); the characteristics of these peptides were similar to those used in our previous study.[13] LC MS-MS of SDS-PAGE enzymatic digests of both peptides confirmed the presence of oligopeptides aligning with HEV-A4 p239 and HEV-C1 p241 sequences with good coverage (Fig. S2). Under electron microscopy, peptides formed pleomorphic virus-like particles (VLPs) of 20–60 nm (Fig. 1C).

Optimisation of IgG EIA assays

We then designed IgG EIAs using HEV-A4 p239 and HEV-C1 p241 coated in microtitre plates. We have previously provided proof-of-concept that immunoblots based on these peptides can differentiate HEV-A and HEV-C1 patient sera although cross-reactivity in HEV-C1 sera occurs.[13] Paired HEV-A4 p239 and HEV-C1 p241 immunoblot data for 33 patients with hepatitis E (21 patients with HEV-A and 12 patients with HEV-C1) are shown in Fig. S3. Immunoblots for a given sample were considered positive if a band was present in the genus-cognate immunoblot. The sensitivity of the immunoblots against HEV RT-PCR was 75.8% (95% CI: 57.7–88.9%) and specificity was 100% (95% CI: 69.1–100%). HEV-C1 samples frequently cross-reacted in HEV-A4 p239 immunoblots, but not *vice versa*. For optimisation of peptide coating concentrations and serum dilution for EIAs, we selected five HEV-A and five HEV-C1 RT-PCR-positive plasma samples from patients. Two of the HEV-C1 that only reacted in the cognate-peptide immunoblot, that is plasma formed bands in the HEV-C1 p241 immunoblot but not in the HEV-A4 p239 immunoblot whereas the other three samples cross-reacted in both immunoblots (Fig. S3B). When HEV-A4 p239 was used as the coating antigen for EIA, cross-reactivity was observed with three HEV-C1 plasma samples from patients corresponding to cross-reactive samples on immunoblot (Fig. 2A). This cross-reactivity dipped when wells were coated with 50 ng of HEV-A4 p239. Robust OD signals for HEV-A plasma were observed at all sample dilutions, but drop in signal strength was noted for some samples at higher dilutions >1:200. For the HEV-C1 p241 EIA, only limited cross-reactivity was observed with HEV-A

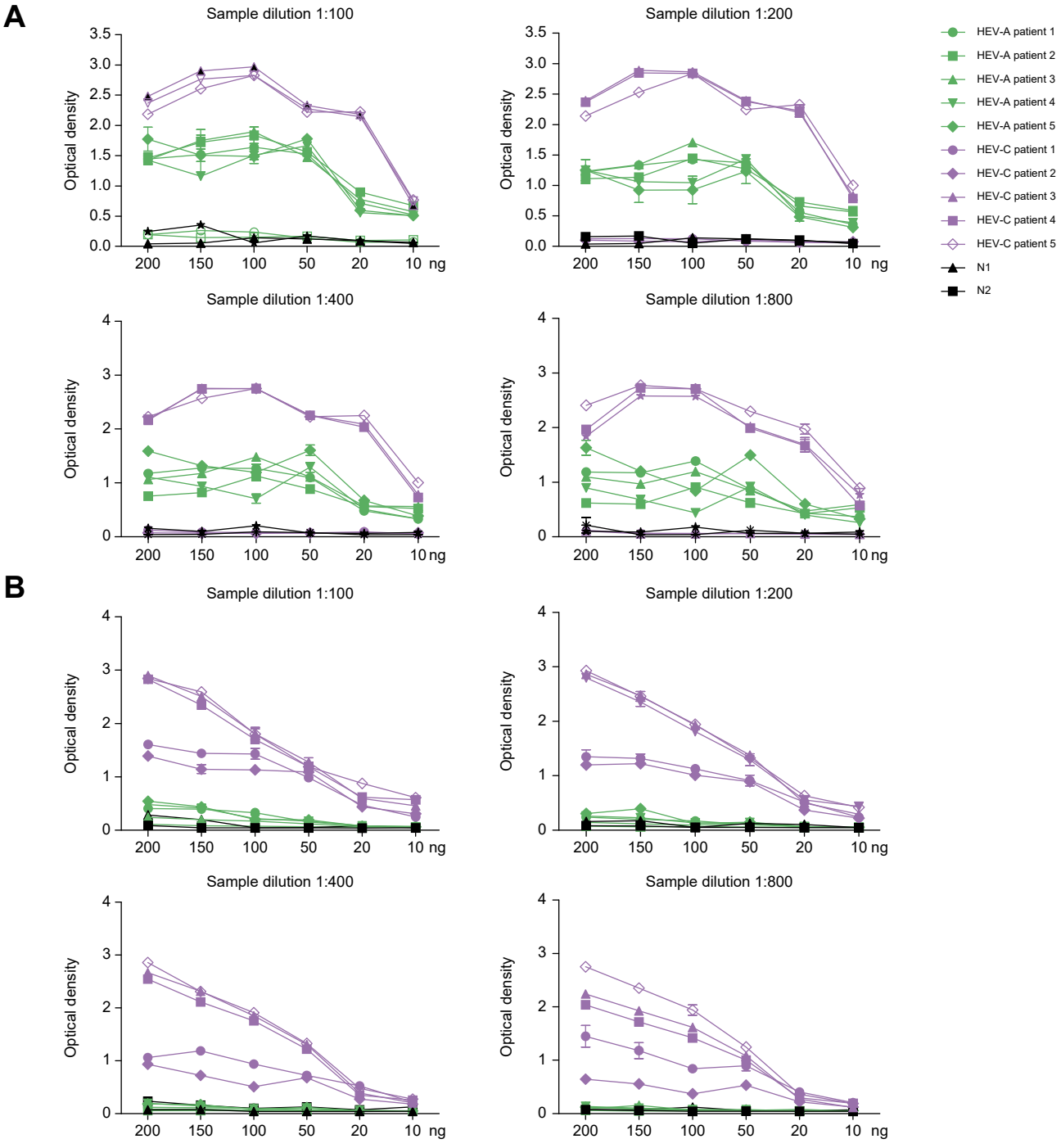

Fig. 2. Optimisation of IgG enzymatic immunoassays (EIAs) using HEV-A4 p239 and HEV-C1 p241. Checkerboard plots of HEV-A4 p239 (A) and HEV-C1 p241 (B) EIAs for optimising antigen coating concentrations and sample dilutions. Five HEV-C1 and five HEV-A RT-PCR-positive plasma samples were chosen for initial EIA optimisation. Two seronegative donor samples served as negative controls. Error bars represent mean and standard deviation of optical densities at denoted antigen coating concentrations and sample dilution. Samples were tested in triplicate. HEV-A, *Paslahepevirus balayani*; HEV-C1, *Rocahepevirus ratti.*

plasma at dilutions of 1:100 and antigen coating >50 ng (Fig. 2B). ODs again dropped off when wells were coated with <50 ng of peptide. Based on these findings, we coated wells with 50 ng of either peptide and diluted samples at 1:200.

Then, 164 sera (obtained from potential organ donors) that were negative in Wantai IgG and both HEV RT-PCR assays were tested in parallel in optimised HEV-A4 p239 and HEV-C1 p241 IgG EIAs to estimate background reactivity. The median OD of these samples was 0.133 in HEV-A4 p239 EIA and 0.115 in HEV-C1 p241 EIA (Fig. S4A; Wilcoxon matched-pairs signed rank test p <0.0001) indicating an acceptable level of noise that was marginally, but significantly, higher in the HEV-A4 p239 EIA. The maximum OD values for these negative control sera in HEV-A4 p239 and HEV-C1 p241 EIAs were 0.388 and 0.235, respectively, and these were taken as 'background thresholds'. Serially diluted WHO reference HEV antisera (0.03–5 U/ml) were tested

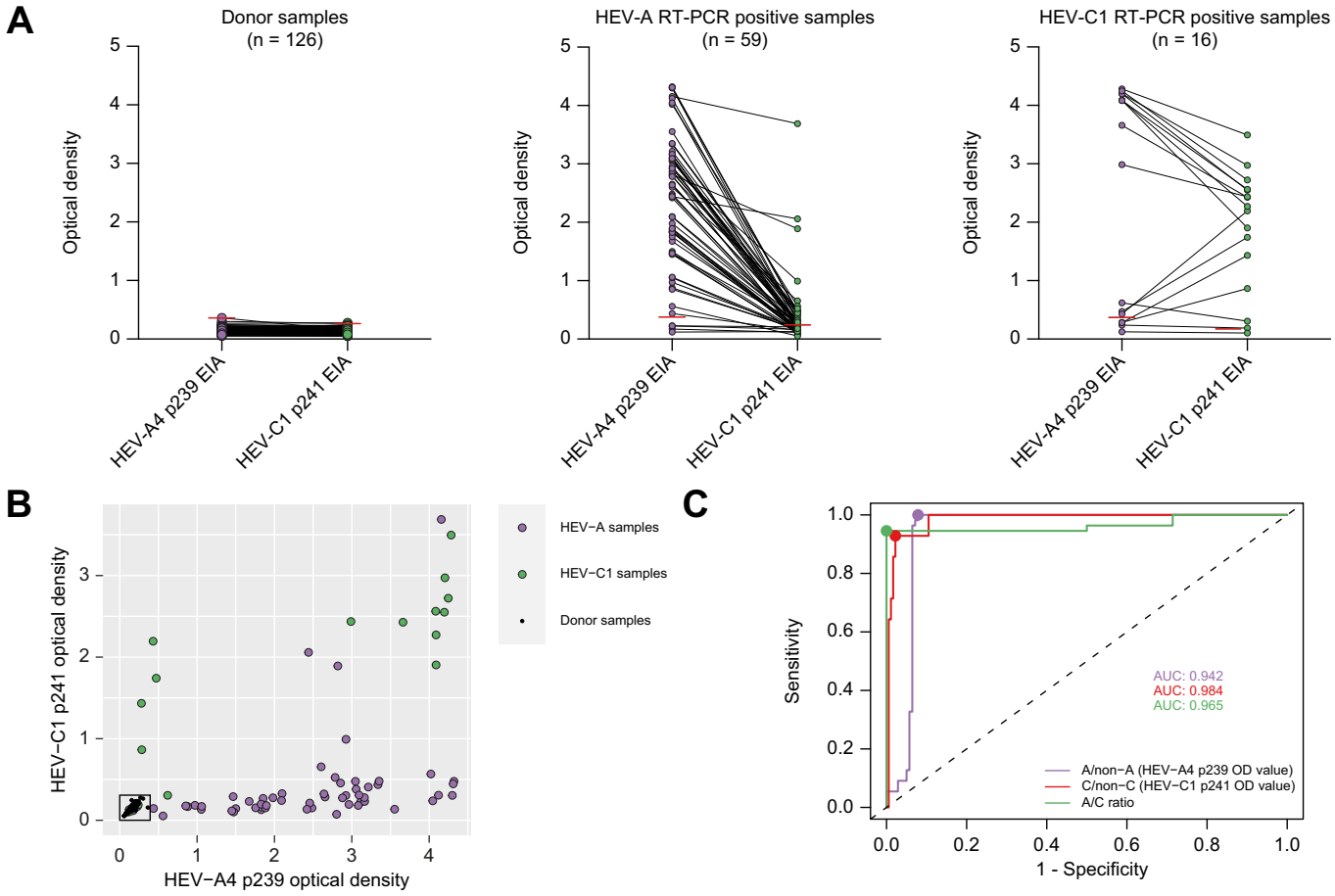

Fig. 3. Optical density (OD) values of hepatitis E patient samples and negative control sera in HEV-A4 p239 and HEV-C1 p241 IgG EIAs. (A) ODs of HEV RT-PCR and Wantai IgG negative donor sera, HEV-A RT-PCR-positive patient sera/plasma, and HEV-C1 RT-PCR positive patient sera/plasma run in parallel in HEV-A4 p239 and HEV-C1 p241 EIAs. Red line represents background thresholds of respective EIAs (0.388 and 0.235 for HEV-A4 p239 and HEV-C1 p241 EIAs, respectively). (B) Two-dimensional scatter plot of HEV-A4 p239 and HEV-C1 p241 OD values showing mostly distinct clusters formed by donor sera, HEV-A RT-PCR positive, and HEV-C1 RT-PCR-positive samples. The cluster formed by the seronegative donor sera is encircled and includes four HEV-A and two HEV-C1 RT-PCR-positive samples that did not show a detectable humoral response in either EIA. (C) Receiver operator characteristic (ROC) curves for establishing cut-offs for individual EIAs and $OD_{HEV\text{-}A4\ p239}/OD_{HEV\text{-}C1\ p241}$ ('A/C ratio'). The blue line is the ROC curve for the HEV-A4 p239 EIA in distinguishing HEV-A and non-HEV-A samples. The red line is the ROC curve for the HEV-C1 p241 EIA in distinguishing HEV-C1 and non-HEV-C1 samples. The green line is the ROC curve for A/C ratios for distinguishing HEV-A and HEV-C1 RT-PCR positive samples. Areas under the curve (AUC) are presented. HEV-A, *Paslahepevirus balayani*; HEV-C1, *Rocahepevirus ratti*; OD, optical density.

in triplicate using Wantai IgG and both EIAs (Fig. S4B). The HEV-A4 p239 EIA generated ODs >0.388 (*i.e.* >background $threshold_{HEV\text{-}A4\ p239}$) for antibody levels as low as 0.03 U/ml; good linearity was observed with R^2 of 0.842. In contrast, all tested antibody concentrations generated much lower ODs in the HEV-C1 p241 EIA; ODs >0.235 (*i.e.* >background $threshold_{HEV\text{-}C1\ p241}$) were only seen at antibody concentrations ≥2.5 U/ml (Fig. S4B).

IgG EIA of samples from patients with hepatitis E

We tested HEV-A and HEV-C1 RT-PCR-positive patient plasma/serum samples in both EIAs. Patients with HEV-C1 tended to be older with higher likelihood of immunosuppression than HEV-A patients (Table 1), which reflects the patient population presenting to clinical attention with HEV-C1 infection.[7] All patients with hepatitis E had active hepatitis at the time of blood collection. Patients with immunosuppressive conditions presented with chronic hepatitis (alanine aminotransferase typically <500 U/L), whereas other patients presented with typical acute hepatitis syndrome (ALT >500 U/L). Characteristics of immunosuppressed patients are described in Table S2. We also tested another 126 Wantai HEV IgG and HEV RT-PCR-negative organ donor sera. HEV-A4 p239 EIA ODs of all patients with HEV-A were higher than their corresponding HEV-C1 p241 ODs (Fig. 3A; p <0.0001 by Wilcoxon matched-pairs signed rank test). Although median HEV-C1 p241 EIA ODs of HEV-C1 patients were much higher than those of HEV-A patients (Fig. S5; p <0.0001 by Mann–Whitney U test), many patients with HEV-C1 also showed robust responses in HEV-A4 p239 EIAs (Fig. 3A). This was expected because several patients with active HEV-C1 infection would inevitably have been exposed to HEV-A in the past given that HEV-A exposure is common in Hong Kong with increasing age.[16] Past HEV-A exposure would not confer immunity to subsequent HEV-C1 infection, but would result in antibody responses to both variants.[13]

To measure intra-assay variance, four HEV-A, four HEV-C1, and four seronegative donor samples were tested in triplicate in both EIA assays. The intra-assay coefficients of variance of HEV-A4 p239 and HEV-C1 p241 EIA ODs were 7.25% and 8.66%,

Table 1. Characteristics of patients whose samples were used for the evaluation of enzymatic immunoassays.

HEV-A (n = 59)*	
Median age in years (interquartile range)	59 (51–66)
Male:female (number of patients)	40:19
Immunosuppressive conditions (n, %)	11 (18.6)
Organ transplant	9
Haematological malignancy	2
Infecting genotype (n, %)	
HEV-A genotype 1	1 (1.7)
HEV-A genotype 3	6 (10.2)
HEV-A genotype 4	47 (79.7)
HEV-A; genotype unknown†	5 (8.4)
HEV-C1 patients (n = 16)*	
Median age in years (interquartile range)	72 (60.5–79)
Male:female (number of patients)	13:3
Immunosuppressive conditions (n, %)	8 (50)
Organ transplant	6
Haematological malignancy	1
Advanced HIV infection	1

HEV-A, *Paslahepevirus balayani*; HEV-C1, *Rocahepevirus ratti*; HIV, human immunodeficiency virus.
* Four HEV-A and two HEV-C1 samples were excluded from final evaluation panel because optical densities were < background thresholds.
† HEV-A RT-PCR positive, sequencing not possible because of low viral load.

respectively. To measure inter-assay variance, two HEV-C1 samples and two HEV-A samples were each tested in triplicate in genus-specific EIAs in four separate runs over 3 days. The inter-assay coefficient of variance of ODs were 9.8% and 9.0% for the two HEV-A samples. The inter-assay coefficient of variance of ODs were 8.7% and 12.2% for the two HEV-C1 samples.

A subset of samples (23 patients with HEV-A and 12 patients with HEV-C1) with sufficient volume remaining were additionally tested in paired HEV-A4 p239 and HEV-C1 p241 IgA EIAs. The results closely matched those of the IgG EIAs with the majority of HEV-A patients having weak HEV-C1 p241 reactive IgA responses (Fig. S5). Many patients with HEV-C1 also cross-reacted with the IgA EIA just like the IgG responses. Results were congruent with the IgG EIA results.

When examined together, HEV-A, HEV-C1, and seronegative donor samples ODs formed well-demarcated clusters on a two-dimensional plot with limited overlap (Fig. 3B) confirming that serological profiles of patients actively infected with HEV-A and HEV-C1 are distinguishable from each other and from negative controls when both EIA results are considered together. Patients with HEV-C1 formed two clusters depending on the strength of their HEV-A4 p239 response.

Samples from four patients with HEV-A and two patients with HEV-C1 generated ODs lower than respective background thresholds in both EIAs (Fig. 3B) suggesting that they had not mounted a humoral response as a result of immunosuppression. These six samples were excluded as they could not contribute to evaluation of cut-offs for differentiating HEV-A and HEV-C1 infection sera. This left behind 55 HEV-A samples and 14 HEV-C1 samples for subsequent cut-off calculations (hereafter termed 'evaluation panel'). We used this panel to design an interpretation algorithm that could differentiate HEV-A and HEV-C1 infection sera/plasma based on their combined results in both EIAs.

Establishing cut-offs for IgG EIAs

We first established interpretation cut-offs for the HEV-A4 p239 EIA as follows. The evaluation panel was split into HEV-A RT-PCR positive (n = 55) and non-HEV-A samples (n = 140, comprising 14 HEV-C1 and 126 organ donor samples). An $OD_{HEV\text{-}A4\ p239}$ cut-off of 0.437 gave the highest Youden index on the receiver operating characteristic (ROC) curve (Fig. 3C). This cut-off gave a sensitivity of 100% (95% CI: 93.5–100%) and specificity of 92.1% (95% CI: 86.4–96%) in differentiating HEV-A and non-HEV-A samples (Table S3). The process was repeated for the HEV-C1 p241 EIA, splitting the evaluation panel into HEV-C1 RT-PCR-positive (n = 14) and non-HEV-C1 samples (n = 181 comprising 55 HEV-A and 126 organ donor samples). An $OD_{HEV\text{-}C1\ p241}$ cut-off of 0.864 gave a sensitivity of 92.9% (95% CI: 66.1–99.8%) and specificity of 97.8% (95% CI: 94.4–99.4%) in differentiating HEV-C1 and non-HEV-C1 samples (Fig. 3C and Table S4). We note that this is a very stringent cut-off for samples diluted 1:200, but this confers the advantage of high specificity in convalescent samples. To differentiate HEV-A and HEV-C1 samples, we assessed the $OD_{HEV\text{-}A4\ p239}/OD_{HEV\text{-}C1\ p241}$ ratio ('A/C ratio') to differentiate HEV-A (n = 55) and HEV-C1 (n = 14) RT-PCR-positive samples. An A/C ratio of 2.947 (*i.e.* A/C ratio ≥2.947 assigned as HEV-A and A/C ratio <2.947 assigned as HEV-C) was able to differentiate HEV-A and HEV-C1 samples with an accuracy of 95.7% (95% CI: 87.8–99.1%) (Fig. 3C, Fig. S6 and Table S5).

Using the above cut-offs, we designed an interpretation algorithm when a sample is run in parallel in both EIAs (Table 2). As shown in the table, interpretation is straightforward when both EIAs are negative or either EIA is positive. When samples test positive in both EIAs (which was the case for most HEV-C1 patients, but only a minority of HEV-A patients), past exposure to both HEV genera is the likely explanation, but A/C cut-off indicates the HEV genus to which the patient is definitely exposed based on our evaluation against a RT-PCR gold standard. The performance of the entire algorithm correlated excellently with the RT-PCR gold standard (Table S6; Cohen's κ = 0.959). Performance parameters for various binary analyses using this interpretation algorithm are presented in Table S7. The overall accuracy of the algorithm in differentiating HEV-A and HEV-C1 samples was

Table 2. Interpretation algorithm for HEV-A4 p239 and HEV-C1 p241 IgG enzymatic immunoassays.

Serum/plasma sample run in parallel in HEV-A4 p239 and HEV-C1 p241 IgG EIAs		
HEV-A4 p239 EIA result (positive if OD ≥0.437)	**HEV-C1 p241 EIA result (positive if OD ≥0.864)**	**Interpretation**
Negative	Negative	Seronegative for hepatitis E
Positive	Negative	Exposure to HEV-A
Negative	Positive	Exposure to HEV-C1
Positive	Positive	Assess A/C ratio*: If ≥2.947, consistent with exposure to HEV-A. Additional HEV-C1 exposure possible. If <2.947, consistent with exposure to HEV-C1. Additional HEV-A exposure possible.

EIA, enzymatic immunoassay; HEV-A, *Paslahepevirus balayani*; HEV-C1, *Rocahepevirus ratti*; OD, optical density.
* A/C ratio = $OD_{HEV\text{-}A4\ p239}/OD_{HEV\text{-}C1\ p241}$.

Table 3. Demographic characteristics and parallel IgG EIA results of SOT and immunocompetent patient cohorts.

	SOT recipients (n = 599)	Immunocompetent (n = 599)
Median age (interquartile range)	57 (48–63)	57 (47–63)
Sex (male:female)	364:235	360:239
Parallel IgG EIA results (n, %)		
Both EIAs negative	545 (91.0)	542 (90.5)
HEV-A4 p239 EIA alone positive	47 (7.8)	53 (8.8)
HEV-C1 p241 EIA alone positive	2 (0.3)	0 (0.0)
Both EIAs positive; A/C ratio consistent with HEV-C1 exposure	5 (0.8)	4 (0.7)

EIA, enzymatic immunoassay; HEV-A, *Paslahepevirus balayani*; HEV-C1, *Rocahepevirus ratti*; SOT, solid organ transplant.

94.2% (95% CI: 85.8–98.4%). Using McNemar's test, we found that our algorithm performed similarly to the Wantai IgG assay in the evaluation panel (p = 0.371). However, we hypothesised that the sensitivity of our parallel IgG EIA system would be lower in convalescent patients because of their waning antibody levels, stringent cut-offs, and relatively high serum dilution of 1:200. We accepted this trade-off to limit false positives.

To investigate the trend in convalescence, we retrieved convalescent samples from 14 individuals in our evaluation panel (eight patients with HEV-A and six patients with HEV-C1). Convalescent samples were obtained at a median of 12 months post-diagnosis (interquartile range: 6–31.5 months). All convalescent samples were HEV RT-PCR negative. Paired EIA results of convalescent sera were assessed using the algorithm in Table 2. The final assignations of 12/14 (85.7%) samples were concordant between acute and convalescent sera. Genus-specific EIA OD values generally declined in convalescence (Fig. S7 and supplementary material), but OD values of most patients with HEV-A and HEV-C1 remained above the cut-off of genus-cognate EIAs. One HEV-A and one HEV-C1 RT-PCR-positive sample turned seronegative after 6 years and 6 months, respectively. Samples from two patients with hepatitis E that were seronegative during the acute phase (because of immunosuppression) also remained seronegative in late convalescence. However, we note that many individuals in this analysis were immunocompromised, which might affect the generalisability of results to the general population.

Seroprevalence in immunocompromised and immunocompetent cohorts

We observed that HEV-C1 infections presenting for clinical attention in Hong Kong disproportionately occurred in immunocompromised patients.[7] Therefore, we tested samples from 599 immunocompromised SOT recipients and 599 age-matched immunocompetent controls using the parallel IgG EIA system. Results were analysed as per Table 2. Patient characteristics and screening results are presented in Table 3. Overall, 54/599 (9.0%) SOT recipients and 57/599 (9.5%) of the immunocompetent individuals were seropositive in either or both EIAs (p = 0.765). The EIA pattern was consistent with HEV-A exposure in 47/599 (7.8%) SOT recipients and 53/599 (8.8%) immunocompetent individuals (p = 0.531). The EIA pattern was consistent with HEV-C1 exposure in 7/599 (1.2%) SOT recipients and 4/599 (0.7%) immunocompetent individuals (p = 0.547). We performed HEV-C1 p241 immunoblot for eight individuals who were seropositive with sufficient residual plasma available, of which six were SOT recipients and two were immunocompetent. All samples produced discernible bands in the HEV-C1 p241 immunoblot with six samples cross-reacting in both immunoblots (Fig. S8).

Characteristics of patients who were HEV-C1 seropositive are described in Table 4. Most were middle aged or elderly. Mild transient biochemical hepatitis was observed in 5/11 (45.5%) individuals. However, not all had regular blood samples taken, so subclinical hepatitis in the remaining six individuals cannot be excluded. HEV-C1 seropositive samples with sufficient sample volume remaining (9/11) were tested by nested HEV-C1 RT-PCR. All patients tested negative on HEV-C1 RT-PCR excluding active infection.

Discussion

HEV-C1 is an emerging cause of hepatitis E with extensive but incomplete antigenic divergence from HEV-A.[13] Accurate serological assays are required to investigate prevalence of HEV-C1 infection in humans. HEV-A4 p239 and HEV-C1 p241 peptides are good candidates for serodiagnostic EIAs because they include most immunogenic epitopes of the native viral capsid.[17] We confirmed that both HEV-A4 p239 and HEV-C1 p241 form VLPs.

Table 4. Characteristics of individuals with parallel IgG EIA results indicating HEV-C1 exposure.

Patient	Age	Sex	Ethnicity	Underlying conditions	HEV-C1 p241 OD value	A/C ratio*	Documented unexplained hepatitis
1	30	M	Chinese	Renal transplant	1.531	N/A	No
2	59	M	Chinese	Renal transplant	2.225	N/A	No
3	50	M	South Asian	Liver transplant	1.338	1.433	No
4	70	M	Chinese	Heart transplant	2.711	1.063	Yes
5	75	M	Chinese	Liver transplant	0.967	0.478	Yes
6	40	F	Chinese	Liver transplant	1.928	1.585	No
7	73	M	Chinese	Heart transplant	1.290	1.290	Yes
8	62	M	Chinese	Diabetes, HBV carrier	0.988	1.278	No
9	70	F	Chinese	Diabetes, HBV carrier	1.719	1.426	Yes†
10	74	M	Chinese	Hypertension	1.500	1.183	Yes
11	61	M	Chinese	HBV carrier	0.925	0.692	No

EIA, enzymatic immunoassay; HBV, hepatitis B virus; HEV-C1, *Rocahepevirus ratti*; N/A, not applicable; OD, optical density.
* A/C ratio = $OD_{HEV\text{-}A4\ p239}/OD_{HEV\text{-}C1\ p241}$ only applied when samples are positive in both EIAs.
† Transient alanine aminotransferase elevation when HBV was suppressed with entecavir.

This feature is likely to improve conformational antigen presentation in the solid phase of EIAs.

Using these two peptides in a parallel IgG EIA format, we describe the first fully validated parallel assay algorithm capable of detecting antibodies against HEV and classifying individuals into HEV-A or HEV-C1 mono-exposed or dual-exposed states. Two earlier studies attempted to detect HEV-C1 antibodies in human sera using EIAs, but these assays were not validated as there were no confirmed human HEV-C1 cases at the time of these studies.[18,19] In contrast, we used an evaluation panel comprising blood samples from the majority of HEV-C1 patients documented to date. This enabled establishment of cut-offs that increased confidence in results when the assay system was applied to test samples from patients with unknown HEV-C1 exposure. Sample dilutions of 1:200, stringent cut-offs, and a validated interpretation algorithm enhanced specificity of the assay. HEV IgA assays have been previously described and we demonstrated that our assay system can also be used to detect and differentiate HEV IgA signatures in samples.[20]

Our parallel IgG EIA algorithm can be deployed conveniently for large-scale seroprevalence studies to map distribution of HEV-C1 infection in humans. This will uncover risk factors for HEV-C1 infection, which are currently poorly understood. We have previously observed that half of all HEV-C1 infections in Hong Kong, a city using population-wide HEV-C1 RT-PCR surveillance, occurred in patients who were immunocompromised.[7] This could either be a result of higher infection incidence in patients who were immunocompromised (because of a lower infectious dose) or a higher chance of presenting to medical attention as a result of more frequent blood taking and closer follow-up. Therefore, we measured and compared HEV-A and HEV-C1 seroprevalence rates in SOT recipients and individuals who were immunocompetent matched for age. The overall measured HEV-C1 seroprevalence of 11/1198 (0.9%) was close to our *a priori* estimate of 1.5% based on the proportion of HEV-C1 to HEV-A RT-PCR-positive cases in Hong Kong. Similar to HEV-A, it is likely that most HEV-C1 infections in humans are asymptomatic.[3] Despite their immunosuppressed state, HEV-C1 IgG seropositivity tended to be higher among SOT recipients than individuals who were immunocompetent, although this did not reach statistical significance. We conclude that the disproportionate burden of HEV-C1 infections in patients who were immunocompromised is mostly because biochemical hepatitis is more likely to be detected and investigated in this population, especially because infections in SOT recipients often become chronic.[6,7]

This study has the following limitations. Our evaluation panel only included 14 HEV-C1 RT-PCR-positive samples. However, this already represents the world's largest repository of HEV-C1 infection sera. Identification of further human HEV-C1 cases will enable us and others to hone assay performance. We evaluated our assay against an RT-PCR gold standard. It is very likely that some patients in the evaluation panel were exposed to both HEV-A and HEV-C1. Concomitant evaluation against a live virus neutralisation assay would have been ideal, but is difficult given the strain-dependent yield of HEV in cell lines.[21] Although a monoclonal antibody neutralisation assay for HEV-C1 has been described in PLC/PRF/5 cells, our experience is that HEV-C1 grows poorly in this cell line.[22,23] Furthermore, even a neutralisation assay would ultimately require comparison against a RT-PCR gold standard. The sensitivity of our parallel IgG EIA in non-viraemic post-acute samples is likely to be low because of high sample dilution. Furthermore, the cut-off of our HEV-C1 EIA was set quite high. These were intentional choices; we hoped to limit false positives as much as possible when applying the EIA system for HEV-C1 serological surveillance. A final limitation was that we did not develop IgM EIAs. Although this is technically feasible, our primary aim was to create an assay for population seroprevalence studies rather than acute illness diagnosis.

In conclusion, we anticipate that this parallel IgG EIA system for detecting and differentiating HEV-A and HEV-C1 IgG antibodies is a valuable tool for gauging prevalence of HEV-C1 infection in humans. We present the first confident estimate of HEV-C1 seroprevalence in the human population using this assay.

Abbreviations

AUC, areas under the curve; EIA, enzymatic immunoassay; HEV-A, *Paslahepevirus balayani*; HEV-C1, *Rocahepevirus ratti*; LC MS-MS, liquid chromatography with tandem mass spectrometry; OD, optical density; ORF2, open reading frame 2; ROC, receiver operating characteristic; RT-PCR, reverse-transcription PCR; SOT, solid organ transplant; VLPs, virus-like particles.

Financial support

This work was supported by the Health and Medical Research Fund (HMRF), Food and Health Bureau, Government of the Hong Kong Special Administrative Region under Grant 20190362; and Health@InnoHK, Innovation and Technology Commission, the Government of the Hong Kong Special Administrative Region.

Conflicts of interest

SS reports provisional patent applications for 'Hepatitis E virus-like particles and uses thereof' covering the utilisation of virus-like particles described in this paper for serodiagnosis and vaccines (US PTO application no. 63/166,698 and PCT application no. PCT/CN2022/081996). The other authors declare no conflicts of interest.

Please refer to the accompanying ICMJE disclosure forms for further details.

Authors' contributions

Conceived and designed the study: SS, Designed the EIA and characterised the peptides: JS, JPC, Established EIA cut-offs: KLHY, Ran EIA experiments: ZL, Genotyped HEV-A isolates: SW, EHKS, Performed transmission electron microscopy: NFSC, Performed data analysis and manual matching: GSMC, WHMC, Retrieved samples for EIA experiments: JYHT, Designed the peptide alignment and phylogenetic tree figures: CCCY, Analysed the LC MS-MS results: KHS, Provided samples for the evaluation panels: VCCC, Critically reviewed the paper: VCCC, KYY.

Data availability statement

Optical densities of the evaluation group and codes for cut-off optimisation and predictive algorithm are included in the following link: https://github.com/lhykelvin/hev-eia. Optical density data for evaluation of assay precision and IgA assays are available upon request.

Acknowledgements

We acknowledge Dr Ken Ho-Leung Ng for providing archived hepatitis E samples from the Department of Health PHLSB for the evaluation. Mass spectrometry analysis was performed at Centre for PanorOmic Sciences – Proteomics and Metabolomics Core Facility, Li Ka Shing Faculty of Medicine, The University of Hong Kong, Hong Kong. The graphical abstract was created using BioRender.com.

Supplementary data

Supplementary data to this article can be found online at https://doi.org/10.1016/j.jhepr.2023.100793.

References

Author names in bold designate shared co-first authorship.

[1] Wang B, Yang X-L. Chirohepevirus from bats: insights into hepatitis E virus diversity and evolution. Viruses 2022;14:905.

[2] Sridhar S, Teng JLL, Chiu TH, Lau SKP, Woo PCY. Hepatitis E virus genotypes and evolution: emergence of camel hepatitis E variants. Int J Mol Sci 2017;18:869.

[3] Kamar N, Bendall R, Legrand-Abravanel F, Xia NS, Ijaz S, Izopet J, et al. Hepat E. Lancet 2012;379:2477–2488.

[4] Sridhar S, Yip CCY, Wu S, Cai J, Zhang AJ, Leung KH, et al. Rat hepatitis E virus as cause of persistent hepatitis after liver transplant. Emerg Infect Dis 2018;24:2241–2250.

[5] Wang B, Harms D, Yang XL, Bock CT. Orthohepevirus C: an expanding species of emerging hepatitis E virus variants. Pathogens 2020;9:154.

[6] Sridhar S, Yip CC, Wu S, Chew NF, Leung KH, Chan JF, et al. Transmission of rat hepatitis E virus infection to humans in Hong Kong: a clinical and epidemiological analysis. Hepatology 2021;73:10–22.

[7] Sridhar S, Yip CC, Lo KH, Wu S, Situ J, Chew NF, et al. Hepatitis E virus species C infection in humans, Hong Kong. Clin Infect Dis 2022;75:288–296.

[8] **Rivero-Juarez A**, **Frias M**, Perez AB, Pineda JA, Reina G, Fuentes-Lopez A, et al. Orthohepevirus C infection as an emerging cause of acute hepatitis in Spain: first report in Europe. J Hepatol 2022;77:326–331.

[9] Andonov A, Robbins M, Borlang J, Cao J, Hattchete T, Stueck A, et al. Rat hepatitis E virus linked to severe acute hepatitis in an immunocompetent patient. J Infect Dis 2019;220:951–955.

[10] Faber M, Wenzel JJ, Erl M, Stark K, Schemmerer M. No evidence for orthohepevirus C in archived human samples in Germany, 2000–2020. Viruses 2022;14:742.

[11] Parraud D, Lhomme S, Péron JM, Da Silva I, Tavitian S, Kamar N, et al. Rat hepatitis E virus: presence in humans in South-Western France? Front Med (Lausanne) 2021;8:726363.

[12] Pankovics P, Némethy O, Boros Á, Pár G, Szakály P, Reuter G. Four-year long (2014–2017) clinical and laboratory surveillance of hepatitis E virus infections using combined antibody, molecular, antigen and avidity detection methods: increasing incidence and chronic HEV case in Hungary. J Clin Virol 2020;124:104284.

[13] Sridhar S, Situ J, Cai JP, Yip CC, Wu S, Zhang AJ, et al. Multimodal investigation of rat hepatitis E virus antigenicity: implications for infection, diagnostics, and vaccine efficacy. J Hepatol 2021;74:1315–1324.

[14] Sridhar S, Lo SK, Xing F, Yang J, Ye H, Chan JF, et al. Clinical characteristics and molecular epidemiology of hepatitis E in Shenzhen, China: a shift toward foodborne transmission of hepatitis E virus infection. Emerg Microbes Infect 2017;6:e115.

[15] Sridhar S, Chew NF, Situ J, Wu S, Chui ES, Lam AH, et al. Risk of hepatitis E among persons who inject drugs in Hong Kong: a qualitative and quantitative serological analysis. Microorganisms 2020;8:675.

[16] Tsoi WC, Zhu X, To AP, Holmberg J. Hepatitis E virus infection in Hong Kong blood donors. Vox Sang 2020;115:11–17.

[17] Zhang J, Li SW, Wu T, Zhao Q, Ng MH, Xia NS. Hepatitis E virus: neutralizing sites, diagnosis, and protective immunity. Rev Med Virol 2012;22:339–349.

[18] Dremsek P, Wenzel JJ, Johne R, Ziller M, Hofmann J, Groschup MH, et al. Seroprevalence study in forestry workers from eastern Germany using novel genotype 3- and rat hepatitis E virus-specific immunoglobulin G ELISAs. Med Microbiol Immunol 2012;201:189–200.

[19] Shimizu K, Hamaguchi S, Ngo CC, Li TC, Ando S, Yoshimatsu K, et al. Serological evidence of infection with rodent-borne hepatitis E virus HEV-C1 or antigenically related virus in humans. J Vet Med Sci 2016;78:1677–1681.

[20] Anastasiou OE, Thodou V, Berger A, Wedemeyer H, Ciesek S. Comprehensive evaluation of hepatitis E serology and molecular testing in a large cohort. Pathogens 2020;9:137.

[21] Fu RM, Decker CC, Dao Thi VL. Cell culture models for hepatitis E virus. Viruses 2019;11:608.

[22] Kobayashi T, Takahashi M, Tanggis, Mulyanto, Jirintai S, Nagashima S, et al. Characterization and epitope mapping of monoclonal antibodies raised against rat hepatitis E virus capsid protein: an evaluation of their neutralizing activity in a cell culture system. J Virol Methods 2016;233:78–88.

[23] Chew N, Situ J, Wu S, Yao W, Sridhar S. Independent evaluation of cell culture systems for hepatitis E virus. Viruses 2022;14:1254.